

# ELIMINATION OF THE RIE 1<sup>ST</sup> WAFER EFFECT: REAL-TIME CONTROL OF PLASMA DENSITY

Pete Klimecky, Jessy Grizzle, and Fred L. Terry, Jr.  
crown@eecs.umich.edu  
University of Michigan/EECS Dept.

## *Abstract*

The wall-state of reactive ion etch tools is known to strongly affect etch results, and previous studies show neutral species concentrations vary with chamber seasoning. In this paper, we show the first reported simultaneous measurements of wall-state-induced plasma density and poly-Si etch rate changes, and demonstrate a real-time feedback control system that corrects for the plasma density variation. This eliminates the “first wafer” effect in Cl<sub>2</sub> etching of poly-Si in a Lam 9400 TCP. Contrasting chamber conditions studied include fluorination/cleaning by C<sub>2</sub>F<sub>6</sub> plasmas vs. chlorination/deposition from Cl<sub>2</sub> plasmas. Transient density changes from opposing wall states were measured using a microwave resonance cavity technique called BroadBand RF. Following chamber fluorination, Broadband data show a significant ( $\geq 20\%$ ) increase in electron plasma frequency during a 60sec Cl<sub>2</sub> etch. Independent sensor measurements correlate strongly with the BroadBand signals, particularly real-time poly-Si etch rate and SiCl<sub>4</sub> etch product concentration. These observed real-time variations were then compensated using a proportional-integral (PI) feedback control algorithm, where BroadBand peak frequency is the control output and TCP power is the controller state variable. Such PI control not only stabilizes BroadBand peak frequencies, but also steadies poly-Si real-time etch rate and SiCl<sub>4</sub> etch product.

## *Keywords*

BroadBand RF, electron density, feedback control, plasma, etch rate, transient effects, wall state, Cl<sub>2</sub>, RIE

## **Introduction**

High yield, high throughput processing is of primary importance in modern semiconductor manufacturing. With current CD design rules shrinking below 0.13 $\mu\text{m}$ , the demand for consistent reactive ion etching (RIE) steps is crucial to increasing overall yield while maintaining high wafer throughput. Though many advances have been made to this end, some of the most useful plasma chemistries (Cl<sub>2</sub> in particular) and process regimes (high density and low pressure) are highly complex, non-linear systems which are poorly modeled physically. This means modern high quality RIE process manufacturing still requires multiple test wafers, frequent plasma clean steps, and frequently scheduled chamber maintenance in order to reduce variance and maintain a consistent manufacturing environment. Tighter controls on the root causes of etch variance would help improve fabrication tolerance limits.

One area of ongoing interest regarding the source of process variations over time is that of the process chamber wall condition [1-6]. Depending on the starting condition of the chamber (either clean or seasoned), Aydil and others have shown significant transient effects on active etch species, such as Cl and Cl<sup>+</sup>[1-4], over time. Different rate limiting reactions at the wall surface have been proposed as reasons for changing Cl concentrations, dependent upon whether an SiO<sub>2</sub> layer has built up over time, or whether the walls have been essentially stripped of oxide layers by means of a previous fluorine containing plasma clean step.

The goal of this project is to demonstrate that, in addition to reactive species dependence on wall seasoning, we have found there are associated plasma density variations which can be attributed to the chamber wall

state, and that these density variations can be compensated using feedback control of the TCP plasma generation power. Our hypothesis maintains that dynamic chemical reactions between plasma species and the chamber walls and quartz top plate have significant transient effects on both active chemical concentrations and measured electron density. We show that stabilizing these density effects with TCP power also stabilizes poly-Si etch rate in  $\text{Cl}_2$  containing plasmas, as well as  $\text{SiCl}_4$  etch product levels.

## Experimental Setup

The high density, low pressure RIE reactor platform for all experiments is a Lam Research TCP 9400SE. The upper chamber transformer coupled plasma generation (TCP) subsystem supplies 13.56 MHz radio frequency (rf) power through a matching network to a planar spiral coil. All experiments etch undoped poly-Si wafers, electrostatically chucked at 650V, with 100W bias forward power. Wafers are loaded through an entrance loadlock to prevent opening the process chamber to atmosphere. However, the wafers themselves may carry trace residual atmospheric water vapor on the surface when loaded.

A custom built real-time data acquisition (DAQ) and control subsystem, running in a LabVIEW<sup>™</sup> environment, is wired in to compliment the original Lam Research I/O boards on the tool. The custom LabVIEW<sup>™</sup> code (referred to as EMACS – Electronics Manufacturing And Control System) records and actuates all relevant input and control signals at a sampling frequency of 4Hz.

In addition to recording standard Lam tool input and output signals (e.g. TCP, bias power, gas flows, pressure), the EMACS platform also incorporates multiple external sensor subsystems into the DAQ environment. Four additional sensor subsystems monitor the process: 1) BroadBand RF [6] peak absorption frequencies indicate changes in the plasma density state in the chamber. 2) Real-Time Spectroscopic Ellipsometry (RTSE) measures *in situ* film thickness and etch rate wafer state data. 3) Fourier Transform InfraRed spectroscopy (FTIR) monitors chemical state of effluent species concentration in the chamber exhaust. 4) Optical Emission Spectroscopy (OES) records glow discharge intensity of characteristic emission lines of various species in the chamber, specifically Cl and Ar at 822.2 and 750.4nm, respectively.

The primary sensor utilized for this project is the BroadBand RF peak resonance absorption sensor. More detailed descriptions of the sensor are available elsewhere [7], but a brief summary of the salient features are listed here for completeness. A small microwave antenna is inserted about 3" into the sidewall of the chamber and is surrounded by a protective quartz sheath. A microwave signal is launched into the chamber cavity, and the reflection coefficient  $|\Gamma|$  is measured over a broad spectrum

of frequencies, as depicted for several cases in figure 1. The reflection coefficient of the absorbed microwave power has specific resonance frequencies dependent upon the chamber geometry and the permittivity of the medium. Figure 1 shows two prominent resonance modes are present for our chamber conditions, labeled  $\omega_{h1}$  and  $\omega_{h2}$ .

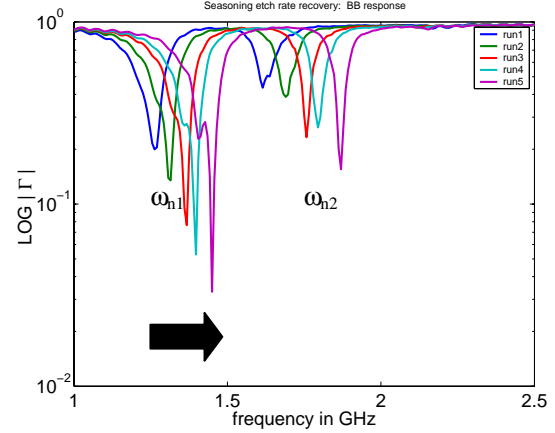


Figure 1. Representative BroadBand peak frequencies showing increasing density with shifts to the right

In particular, Slater [8] and Haverlag [9] have shown these resonance frequencies will shift in the presence of a plasma, because the plasma density influences the medium permittivity [10]. Moreover, the plasma density can be determined from Slater's perturbation formula if geometric factors are idealized and conditions are such that the plasma is collisionless (e.g.  $v_m \ll \omega_p$ ) and the plasma frequency is much less than the empty chamber resonance frequency,  $\omega_p \ll \omega_0$ . Under these conditions, frequency shifts,  $\Delta\omega$ , with and without plasma presence can be related to plasma frequency as,

$$\frac{\Delta\omega}{\omega_0} = \frac{1}{2\omega_0^2} \frac{\iiint_r \omega_p^2 |E|^2 d^3r}{\iiint_r |E|^2 d^3r}. \quad (1)$$

Here, E is the unperturbed resonance electric field,  $\omega_0$  is the empty chamber resonance,  $\omega_p$  is the plasma density, and the integrals are over the entire cylindrical cavity volume with radius r. Due to the plasma frequency dependence on electron density,

$$\omega_p^2 = \frac{n_e q^2}{m_e \epsilon_0}, \quad (2)$$

the density,  $n_e$ , can then be determined from such a relation under certain conditions. Here q is fundamental charge,  $\epsilon_0$  the permittivity of vacuum, and  $m_e$  the electron mass.

Regardless of the idealized features required for Slater's density analysis however, for a given geometry, small perturbations in resonance peak frequency are similarly observed in the presence of two different plasma

conditions, and these frequency shifts can still be attributed to changes in plasma density. This is the relevant point for the purposes of this paper. It has been shown previously [11] that shifts to higher frequencies indicate comparatively higher electron density, and shifts lower indicate lower densities. This point is illustrated with a simple 1D Drude model of the plasma used to simulate resonant modes at different densities, as shown in figure 2.

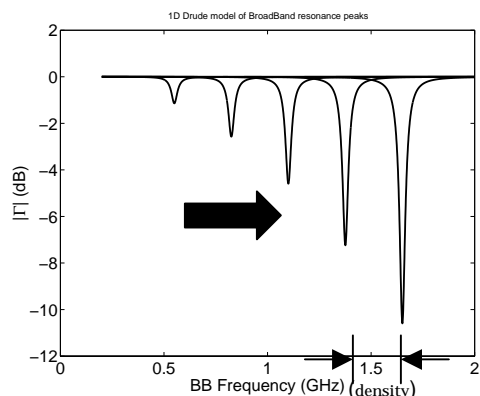


Figure 2. 1D Drude simulation of BroadBand absorption peaks modeled at five different electron densities. Peaks shift right at higher density.

We find that several plasma factors influence the overall shape of the reflection coefficient signal, but only plasma frequency is responsible for the peak resonance position with such a model. Thus we attribute changes in BroadBand peak frequency to plasma density changes.

## Experimental Goals

The primary intent of this project is to demonstrate observed density transients in standard poly-Si etch  $\text{Cl}_2$  plasmas, and then, by relating these changes to the starting wall states and final etch performance results, correct for these density variations using a real-time feedback controller. To accomplish this, three primary experiments are performed: 1) seasoned chamber chlorine etches to establish steady state conditions, 2) open loop control (i.e. uncontrolled) recovery from a non-seasoned chamber to observe transient behavior, and 3) closed loop control recovery from a non-seasoned chamber to observe transient effect compensation.

For experiment 1, we first monitor and establish stable, seasoned etch conditions where all recorded signals have essentially normalized during long running  $\text{Cl}_2$  plasmas, thus establishing "nominal" etch conditions. The stable, nominal chlorine etch chamber state is referred to as the Cl-prep condition. This nominal preparation step required recording stable poly-Si etch rates, constant BroadBand peak frequencies, steady  $\text{SiCl}_4$  FTIR signals, and unchanged OES intensities. The nominal process

recipe used for Cl-prep was 250W TCP, 100W bias, 10mT pressure, and 100sccm  $\text{Cl}_2$  flow with 5% Ar.

Once these Cl-prep conditions are achieved for reference, the wall conditions are perturbed using a short (30sec)  $\text{C}_2\text{F}_6$  plasma recipe to alter the wall state of the chamber. The chamber state after a fluorine treatment is referred to as an F-prep condition.

Following an F-prep, the second test involved a new poly-Si etch with identical chlorine plasma input conditions as used to establish the nominal etch. Sensor signal drifts over time due to the previous F-prep step were recorded, if any. This is an uncontrolled, open loop recovery of the chamber from F-prep back to Cl-prep. Any observed transient signals were found to eventually stabilize back to steady state nominal Cl-prep conditions if the recovery plasma was allowed to run long enough.

Lastly, the third test incorporated a PI feedback control algorithm in the system. As with the second test, a 30s F-prep plasma was performed in the chamber prior to the Cl recovery etch to place the chamber in an unseasoned state, and the chlorine etch recipe is then initiated on a poly-Si wafer. Now, however, the controller used BroadBand peak frequency (indicating plasma density) as the control system output variable to stabilize, and TCP input power as the actuator input variable to normalize the density. The target closed loop setpoint frequency value is the original peak absorption frequency recorded from the nominal Cl-prep. As with the open loop test, the etch proceeded for the specified time while etch product variables are measured for performance improvements. Variability in etch rate, BroadBand frequency position, rf tuning values,  $\text{SiCl}_4$  and OES levels were compared in real-time vs the uncontrolled values measured from the second test. Values were also compared with nominal signals from the first test.

## Experimental Results

The upper plot of Figure 3 shows a real-time comparison between nominal etch rate in a stable Cl-prep chamber and the uncontrolled open loop etch rate recovery which started from an F-prep chamber. The lower plot of figure 3 shows a similar comparison for the corresponding density indicator (the second BroadBand peak frequency  $\omega_{r2}$ ) to open loop recovery peak position. Note the significant drop in both etch rate and density at the start of the open loop runs. Clearly the F-prep step to remove halogenated oxides from the chamber surfaces has a large effect on plasma density as well as plasma chemistry. In the 60s time allotted for the open loop etch, the BroadBand frequency and etch rate did not have sufficient time to fully recover to their respective nominal values. Other tests show full recovery time back to nominal Cl-prep conditions of ~5mins is required using the nominal recipe.

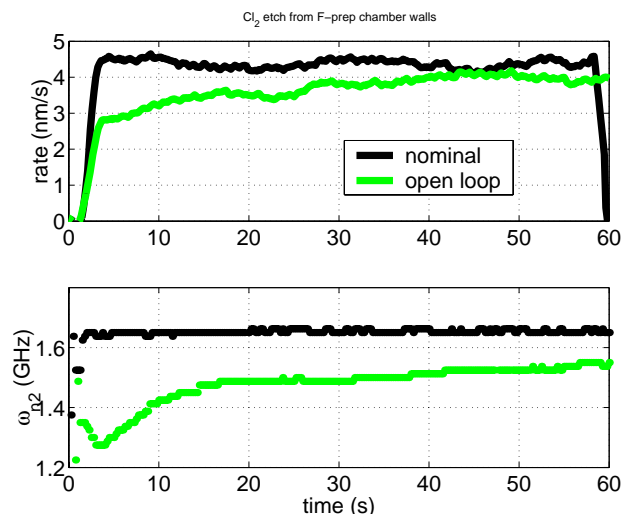


Figure 3. Nominal etch rate vs open loop recovery & BroadBand peak frequency nominal vs open loop

By contrast, figure 4 shows nominal etch rate again, only now compared to closed loop etch rate in the top plot, while corresponding  $\omega_{B2}$  peak is compared in the lower plot. With minimal initial overshoot, we see the density recovery time is drastically reduced and the corresponding real-time etch rate is also leveled out.

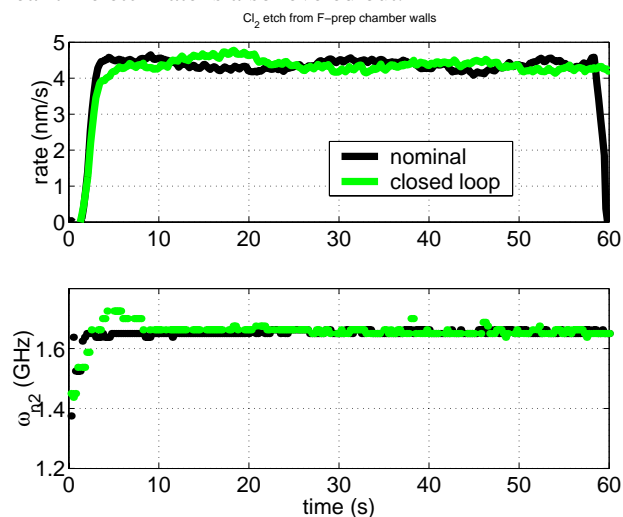


Figure 4. Nominal etch rate vs closed loop recovery & BroadBand peak frequency nominal vs closed loop

Utilizing the FTIR system to measure etch product species in the foreline exhaust, we find similar behavior with relative concentration of  $\text{SiCl}_4$ . Figure 5 compares  $\text{SiCl}_4$  levels for the same three etches. Note the suppression of  $\text{SiCl}_4$  early in the open loop etch due to Cl species loss to the walls. Conversely, the closed loop etch compensates for the density loss to the walls with proportionally higher TCP power, and thus quickly raises the  $\text{SiCl}_4$  level back close to the nominal point. The overall concentration is also more steady throughout the etch with closed loop compensation.

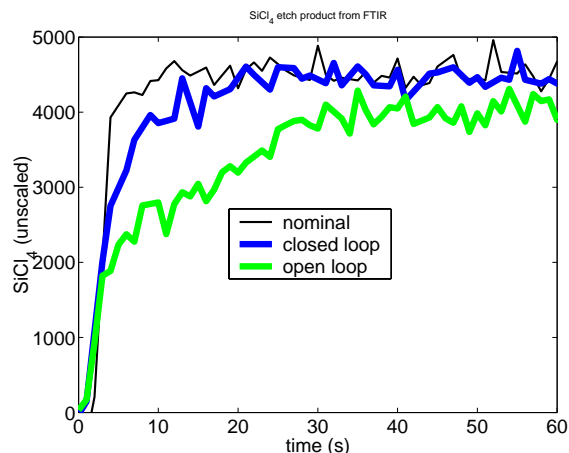


Figure 5. Relative concentration of  $\text{SiCl}_4$  etch product

## Conclusions

We have shown that real-time poly-Si etch rate variations in an industry-standard etch process correlate with plasma density changes. These transient effects are believed to be due to dynamic chamber wall states that affect both Cl neutral concentration as well as electron density. We implemented a real-time feedback controller that corrects for plasma density changes by adjusting TCP power. This system greatly reduces the variations in etch rate and  $\text{SiCl}_4$  effluent concentration. Suppression of the first-wafer effect by this technique could be used to both increase throughput and reduce variance in etch processes.

## Acknowledgements

Thanks to Dr. Jay Jeffries and Suhong Kim at Stanford University for discussion and additional work in support of this project. This work was supported in part by AFOSR/ARPA MURI Center under grant #F49620-95-1-0524 and NIST ATP #70NANB8H4067.

## References

- [1] E. Aydil et al, *JVSTA*, **20**, No. 1 (Jan/Feb 2002)
- [2] V. M. Donnelly, *JVSTA*, **14**, No. 4, pp 1076 (1996)
- [3] G. I. Font et al, *JVSTA*, **16**, No. 4 (Jul/Aug 1998)
- [4] G. Zau & H. Sawin, *J.El.Chem.Soc.* **139**:250-6 (1992)
- [5] A. Watts & W. Varhue, *Appl. Phys. Let.*, **61**,5 (1992)
- [6] M. Malyshev and V. M. Donnelly, *J. Appl. Phys.*, **88**, pp 6207 (2000)
- [7] C. Garvin, D. Grimard, J. Grizzle, *Char & Metrology for ULSI Tech.*, Vol. 449, AIP Press pp 442-6 (1998)
- [8] C. Garvin & J. Grizzle, *JVSTA*, **18**, 4 (Jul/Aug 2000)
- [9] J. C. Slater, *Rev. Mod. Phys.* **18**, No. 4, 441 (1946)
- [10] M. Haverlag et al, *Plasma Chemistry and Plasma Processing*, Vol. 11, No. 3, (1991)
- [11] M. A. Biondi and S. Brown, *Phys. Rev.* **75**, No. 12, pp 1700-1705 (1949)
- [12] P. Klimecky and C. Garvin, *Proc. AEC/APC XII Symposium*, (2000)